ORIGINAL RESEARCH

# Dexamethasone inhibits the proliferation of tumor cells

Yuantao Wu[1]
Rui Xia[1]
Chungang Dai[2]
Suji Yan[2]
Tao Xie[2]
Bing Liu[2]
Lei Gan[1]
Zhixiang Zhuang[1]
Qiang Huang[2]

[1]Department of Oncology, The Second Affiliated Hospital of Soochow University, Soochow, China; [2]Department of Neurosurgery, The Second Affiliated Hospital of Soochow University, Soochow, China

**Objective:** Dexamethasone (DEX) is a glucocorticoid that is commonly used in clinics. Previously, DEX has been shown to inhibit the function of immune system; however, DEX is often used to treat side reactions, such as nausea and vomiting caused by chemotherapy in clinics. Therefore, it is necessary to study the role of DEX in the treatment of cancer.

**Methods:** The effects of DEX on HepG2 were studied in vitro by Cell Counting Kit-8 method, cell cycle, and scratch test. The transplanted tumor model of HepG2 was established in nude mice to study the anti-tumor effect of DEX in vivo. In addition, in order to study the effect of DEX on the immune system, we also established a transplanted tumor model of 4T1 in normal immunized mice to study treatment effect and mechanism of DEX in mice of normal immune function.

**Results:** The results showed that DEX inhibited the proliferation of HepG2 in vitro and in vivo, affecting the cycle and migration of HepG2 cells, and the expression of c-Myc and the activation of mTOR signaling pathway were inhibited. The expression of key enzymes related to glucose metabolism is altered, especially that of phosphoenolpyruvate carboxykinase2 (PCK2). In normal immunized mice, DEX also inhibits the proliferation of tumor cells 4T1, while the proportion of CD4+CD45+T cells and CD8+CD45+ T cells in CD45+ cells in the lymph nodes upregulated, the proportion of Treg cells in CD4+ T cells downregulated in lymph nodes, and the proportion of MDSCs in tumor tissues downregulated.

**Conclusion:** DEX can inhibit tumor cells in vitro and in vivo. The mechanism is to inhibit the activation of mTOR signaling pathway by inhibiting the expression of c-Myc, further affecting the expression of key enzymes involved in glucose metabolism, especially PCK2.In addition, DEX has an inhibitory effect on the immune system, which may be the reason why DEX still has anti-tumor effect in normal mice.

**Keywords:** dexamethasone, glycolysis, Warburg effect, HepG2, 4T1, immune cells, immune system

## Introduction

With the continuous deepening of tumor research, the six basic characteristics of tumors have been expanded to ten, including the addition of the following characteristics: avoiding immune destruction, tumor-promoting inflammation, deregulating cellular energetics, and genome instability and mutation.[1] Warburg first discovered that the enhanced phenomenon of aerobic glycolysis in tumor cells is considered a metabolic marker of malignant tumor cells. The glycolysis process can produce a large number of metabolic intermediates, such as nucleic acids, amino acids, and lipid molecules, to satisfy the need for rapid proliferation in tumor cells.[2] In addition to the three-step

Correspondence: Zhixiang Zhuang
Department of Oncology, The Second Affiliated Hospital of Soochow University, No. 1055, Sanxiang Road, Gusu District, Soochow, 215004, China
Email sdfeyzzx@sina.com

key enzyme-catalyzed steps, the gluconeogenesis process can be understood as a reverse reaction of glycolysis, which can compete with glycolysis for substrates, thereby affecting the material needs of tumor cells during rapid proliferation. Phosphoenolpyruvate carboxykinase is divided into mitochondrial phosphoenolpyruvate carboxykinase (PCK2) and cytoplasmic phosphoenolpyruvate carboxykinase (PCK1), which are the first key enzymes of gluconeogenesis. Their upregulation can catalyze the conversion of oxaloacetate to phosphoenolpyruvate for gluconeogenesis.[3] Liu et al found that PCK2 is involved in the proliferation of hepatoma cells by whole exon sequencing.[4] Meng-Xi Liu et al found that the expression of PCK1 and PCK2 is downregulated in primary hepatoma cells, which is related to poor prognosis in patients. Primary hepatoma can be treated by activating PCK1.[5] Shi also found downregulated expression of PCK1 in hepatoma cells, and the oncoprotein, hepatitis B X-interacting protein(HBXIP), can promote liver cancer by inhibiting PCK1.[6] Other proteins that are associated with glucose metabolism in tumor cells, such as lactate dehydrogenase A (LDHA), are the catalytic enzymes in the last step of aerobic glycolysis and have carcinogenic effects in prostate cancer.[7]

The tumor-associated immune cells around the tumor tissue include not only CD4+ T cells, CD8+ T cells, and natural killer (NK) cells, which promote the anti-tumor effect of the body's immunity, but also myeloid-derived suppressor cells (MDSCs), Tregs (Regulatory T cells), and other cells that inhibit the body's immunity and thus, contribute to tumor growth. To what extent these immune cells play a role in the body has a major impact on the occurrence, development, and outcome of tumors.[8]

Dexamethasone (DEX) was shown to inhibit the function of immune system and affect the glucose metabolism, and DEX is often used to treat side reactions, such as nausea and vomiting caused by chemotherapy in clinics, so we chose DEX as the research object. The liver is the most important organ regulating blood sugar concentration and is the most important organ of gluconeogenesis, so we chose human hepatoma cell line HepG2.

## Materials and methods
### Materials
HepG2 was purchased from the Shanghai Cell Bank of the Chinese Academy of Sciences, 4T1 was purchased from the University of Pittsburgh Medical Center, and DEX was purchased from Anhui Fengyuan Pharmaceutical Co., Ltd. Fluorescent nude mice and BALB/c mice were provided by the Experimental Animal Center of Soochow University.

Individual ventilated caging (IVC) mice were independently supplied with air. The feeding system was purchased from Soochow Suhang Equipment Co., Ltd.; DMEM medium and RPMI-1640 medium were purchased from HyClone, Logan, UT, USA; the fluorescence microscope was purchased from Zeiss, Oberkochen, Germany; fluorescent lights and lenses were purchased from Nightsea, Lexington, MA, USA; the frozen slicer was purchased from Leica, Buffalo Grove, IL, USA; and the flow cytometer was purchased from Beckman CytoFLEX, Krefeld, Germany.

### Animal rearing
Foxn1nu.B6-CAG-EGFP|SU homozygous nude mice, that were 6–8 weeks old, were housed in a mouse IVC system at a ratio of 1:3 to heterozygotes. Hairy female rats were identified under fluorescent flashlight-eyeglasses with strong green fluorescence and were then caged and then continuously reared in the IVC. Four to six weeks old nude female mice and hairy female mice weighing about 20 g were used for experiments, four mice per group.

### Resuscitation and culture of HepG2 cells and 4T1 cells
HepG2 cells and 4T1 cells were taken out from the liquid nitrogen tank, HepG2 cells were cultured in DMEM (Hyclone) supplemented with 10% FBS (BI). The 4T1 cells were cultured in RPMI-1640 medium (Hyclone) supplemented with 10% FBS (BI) and placed in a 37°C, 5% $CO_2$ incubator for culture. After the cells attached themselves to the wall, the solution was changed, passaged, and observed.

### Cell Counting Kit-8 (CCK-8) detects the effects of different concentrations of DEX on the proliferation of HepG2 cells
CCK-8 is based on WST-8 (2-(2-methoxy-4-nitrophenyl)–3-(4-nitrophenyl)–5-(2,4-disulfobenzene)-2H-tetrazole monosodium salt) and is a rapid and highly sensitive detection kit widely used for cell proliferation and cytotoxicity. Its working principle is as follows: in the presence of an electron coupling reagent, it can be reduced by dehydrogenase in the mitochondria to produce a highly water soluble orange–yellow formazan product (formazan). The depth of color is directly proportional to the proliferation of cells and inversely proportional to cytotoxicity. The OD value was measured at a wavelength of 450 mM using a microplate reader, indirectly reflecting the number of viable cells. Plating: HepG2 cells grown to the log phase were inoculated into 96-well cell culture plates at 4,000 per well, which was placed in the cell

incubator. Treatment: After 24 hours, the cells were treated with DEX at 0, 25, 50, 100, 150, 200, 250, 300, 400, and 500 μg/mL, and then placed in a cell incubator for 48 hours. Absorbance value detection: We thoroughly mixed CCK-8 with fresh medium at 1:10. Discarded the medium and added 100 μL of CCK-8 reagent and fresh medium mixture to each well. After incubating for 2 hours in a 37°C incubator, the absorbance values were measured at a wavelength of 450 nm under a full-wavelength microplate reader, and statistical analysis was performed, experiment repeated three times.

## Fluorescence quantitative PCR was used to measure the change of mRNA level after DEX treatment

Plating: HepG2 cells grown to the log phase were counted. About $4 \times 10^5$ cells per well were seeded in a 6-well cell culture plate, which was placed in a cell incubator culture Treatment: 24 hours later, the cells were adhered in the control group, and the medium was replaced with fresh DMEM high glucose and RPMI-1640 medium containing 10% FBS. The DEX group was treated with DMEM high glucose medium containing 300 μg/m DEX and 10% FBS, and then placed in the cell incubator. After 48 hours, total RNA was extracted by the Trizol method, and cDNA was synthesized by reverse transcription kit. The cDNA samples of the control and DEX groups were, respectively, configured with reaction system of internal reference gene and target gene, and each reaction tube was equipped with three auxiliary holes. The prepared PCR reaction solution was placed in a fluorescence quantitative PCR machine for PCR amplification reaction. The reaction conditions were as follows: predenaturation at 95°C for 2 minutes, followed by 95°C for 30 seconds, 55°C for 1 minute (collecting the fluorescent signal), and 72°C for 1 minute, for a total of 45 cycles, experiment repeated three times.

Primers used as below:

Sequence (5′-3′)
LDHA forward primer ATGGCAACTCTAAAGGATCAGC
Reverse primer CCAACCCCAACAACTGTAATCT
PCK1 forward primer AAAACGGCCTGAACCTCTCG
Reverse primer ACACAGCTCAGCGTTATTCTC
PCK2 forward primer GCCATCATGCCGTAGCATC
Reverse primer AGCCTCAGTTCCATCACAGAT
PDK4 forward primer GGAGCATTTCTCGCGCTACA
Reverse primer ACAGGCAATTCTTGTCGCAAA
c-Myc forward primer ATGCCCCTCAACGTCAGCTT
Reverse primer CTTATGCACAAGAGTTCCGTAGCT

Granzyme B forward primer CATGGCCTTACTTTCG ATCAAG
Reverse primer CTCCTGTTCTTTGATGTTGTGG
IFN-γ forward primer GCCACGGCACAGTCATTGA
Reverse primer TGCTGATGGCCTGATTGTCTT
IL-10 forward primer CTTACTGACTGGCATGAGGATCA
Reverse primer GCAGCTCTAGGAGCATGTGG
IL-1B forward primer GAAATGCCACCTTTTGACAGTG
Reverse Primer TGGATGCTCTCATCAGGACAG

## The change in lactic acid content in the medium after DEX treatment was determined

The plating method and the dosing treatment method were the same as those used for PCR. After 48 hours of DEX treatment, the culture medium of the control group and the DEX treatment group were separately collected in 1.5 mL eppendorf tubes, and in each of the three subholes. Dead cells and cell debris were removed by centrifugation at 1,000 rpm for 10 minutes. Two μL of distilled water was added to the blank tube, along with 100 μL of enzyme working solution and 20 μL of color developing solution, and 2 μL of standard solution and 100 μL of enzyme working solution were added to the standard tube. To the control group and the DEX treatment group, we added 2 μL medium, 100 μL enzyme working solution, and 20 μL coloring solution (three subwells were set in each group), and the water bath at 37°C accurately reflected 200 μL in each tube after 10 minutes. We then determined the OD value of each tube at a wavelength of 530 nm, and the lactic acid content of the medium was calculated according to the following formula: C lactic acid (mmol/L) =3 mmol/LX (OD sample–OD blank)/(OD standard–OD blank); the experiment was repeated three times.

## HepG2 subcutaneous transplantation and treatment

All experimental procedures were approved by Ethics Committee of Soochow University and performed according to the guidelines (Guide for the care and use of laboratory animals). HepG2 cells ~$8 \times 10^6$ cells/50 μL PBS were used. The penicillin skin test needle was directly inoculated into the right forelimb of the right side of the nude mouse. When the tumor grew to a diameter of 8 mm, the tumor-bearing mice were divided into control and DEX groups. Each mouse in the DEX group was intraperitoneally injected with 5 μg/g DEX for 18 days. During the treatment, the short diameter (a) and long diameter (b) of the tumor were measured with Vernier

calipers every 3 days. The tumor volume was calculated as follows: $W=a^2\times b/2$. The tumor volume increase curve was then plotted, experiment repeated three times.

## 4T1 subcutaneous transplantation and treatment

All experimental procedures, including the use of 4T1 cells were approved by Ethics Committee of Soochow University and performed according to the guidelines (Guide for the care and use of laboratory animals). When 4T1 cells were in the logarithmic growth phase, $\sim2\times10^5$ cells/50 μL PBS was used. The penicillin skin test needle was directly inoculated into the right mammary gland of the hairy mother. When the tumor grew to a diameter of 5 mm, the tumor-bearing mice were divided into the control group and the DEX group. The grouping principle was the tumor size between the two groups. There was no significant difference in statistical analysis. Each mouse in the DEX group was intraperitoneally injected with DEX 5 μg/g for 18 days. During the treatment, the short diameter (a) and long diameter (b) of the tumor were measured with Vernier calipers every 3 days. The tumor volume was calculated as follows: $W = a^2\times b/2$. The tumor volume increase curve was then plotted, experiment repeated three times.

## Flow cytometry

On the 14th day, two mice in the experimental group and the control group were sacrificed and the experiment was performed. Tumor tissue was taken from each mouse, along with spleen tissues and the lymph nodes near the tumor. The tumor tissue was fully shredded, 1 mL of medium and 20 μL of collagenase was added, followed by incubation at 37°C for 1 hour, transfer to a Petri dish and thorough grinding, filtering through two filters to a centrifuge tube, centrifuging at 1,200 rpm for 5 minutes, discarding the supernatant, and incubating 1 mL. The spleen tissue was placed in a Petri dish, 2 mL of the medium was added, and 2 mL of red blood cell lysate was added after grinding. After lysis for 1 minute, 4 mL of the medium was diluted, and the liquid in the culture dish was transferred to a centrifuge tube through a sieve. After centrifugation at 1,200 rpm for 5 minutes, the supernatant was discarded, and 1 mL of the medium was resuspended; the lymph node tissue was placed in a Petri dish, 2 mL of the medium was added, and after grinding, the liquid in the Petri dish was transferred to a centrifuge tube through a sieve, centrifuged at 1,200 rpm for 5 minutes, and discarded. Cells were resuspended in 1 mL medium and labeled with the appropriate antibody; antibody label: group

A: Gr-1 Fitc, CD11b APC; group B: CD45 Fitc, CD4 PCP, CD8 PC7, FoxP3 PE; group C: CD19 Fitc, DX5 APC, F480 PCP5.5. In addition to FoxP3, we added 2 μL of antibody to 100 μL cells, incubated in the dark for 30 minutes on ice, and resuspended the medium in group A and group C after centrifugation for flow detection. After centrifugation in group B, 400 μL fixative was added on ice for 1 hour. After centrifugation, the supernatant was discarded, 200 μL of ruptured solution was added, cells were resuspended and then centrifuged, 100 μL of rupture solution and 2 μL of FoxP3 antibody were added, followed by incubation for 40 minutes on ice, and 200 μL of membrane rupture solution was then added after centrifugation. After clearing, 400 μL of the medium was resuspended and subjected to flow detection, experiment repeated three times.

## Statistical processing

The volume and mass of the transplanted tumor, the OD value, and the relative expression amount of the fluorescent quantitative PCR were subjected to *t*-tests using GraphPad Prism 7 software.

## Result

## DEX inhibits the proliferation and migration of HepG2 cells

Different degrees of DEX treatment of HepG2 cells for 48 hours inhibited the proliferation of HepG2 cells. When the DEX concentration was 25 μg/mL, there was no significant difference between the DEX group and the control group. When the concentration of DEX was 50 μg/mL, the difference between the DEX group and the control group was statistically significant (Figure 1A). According to the inhibition rate of HepG2 cell proliferation by different concentrations of DEX, the IC50 (50% inhibitory concentration) of DEX was 329 μg/mL by linear fitting. Therefore, 300 μg/mL of DEX was selected for the next experiment (Figure 1B). The CCK-8 experiment showed that the proliferation of HepG2 cells in the control group was significantly enhanced compared with that of the DEX group and was statistically significant on the second day (Figure 1C). HepG2 cells were observed under a microscope after DEX treatment, and the morphology of the cells was changed. Considering that DEX treatment may affect the cell cycle of HepG2, we divided HepG2 cells into a control group and a DEX group, and we harvested cells in the logarithmic growth phase. Analysis showed that the proportion of cells in the G2-M phase of the control group was significantly higher than that of the cells in the G2-M phase of the DEX group. The difference between the two
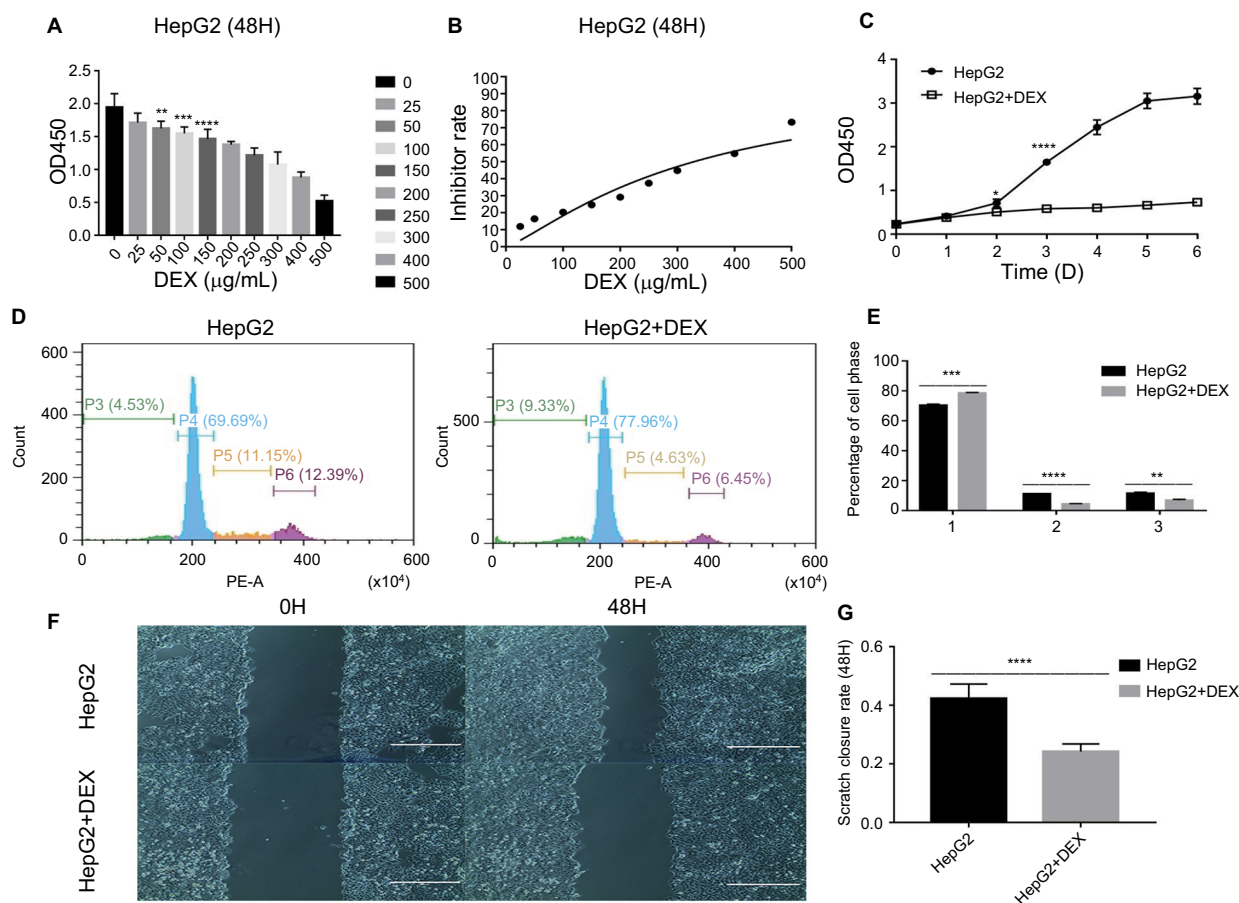
**Figure 1** DEX inhibits proliferation and migration of HepG2 cells in vitro.

**Notes:** Inhibition of HEPG2 cells by different concentrations of DEX. The concentration of DEX is >50 µg/mL, and the inhibition effect is statistically significant (**A**). IC50 fitting curve of DEX, the IC50 of DEX was 329 µg/mL (**B**). Proliferative curve of inhibition of HEPG2 cells by 300 µg/mL DEX. After 2 days of treatment, the proliferation of the two groups of cells was statistically significant (**C**). Flow diagram and statistical diagram of the inhibit effect of DEX on HEPG2 cell cycle. After treatment with DEX, the proportion of cells in the G2/M phase of HepG2 cells was significantly downregulated, and the difference was statistically significant, indicating that DEX can inhibit the proliferation of HepG2 cells (**D** and **E**). Scratch test and statistical diagram of DEX inhibiting the migration ability of HEPG2 cells. After DEX treatment, the scratch closure rate of HepG2 cells was significantly reduced, and the difference was statistically significant, indicating that DEX can inhibit the migration ability of HepG2 (**F** and **G**). All data were analyzed by using chi-squared test. $P<0.05$ was considered to be significant (*$P<0.05$, **$P<0.01$, ***$P<0.001$, ****$P<0.0001$).

**Abbreviation:** DEX, dexamethasone.

groups was statistically significant (Figure 1D, E). Through the cell scratch test, we found that the HepG2 cells were delineated after DEX treatment. The rate of scar closure was significantly reduced, and the difference was statistically significant (Figure 1F, G).

## DEX inhibits tumor growth of HepG2 tumors in vivo

To verify whether DEX has the same effect of inhibiting tumor proliferation that was observed in vitro, we injected human hepatoma cell HepG2 cells into nude mice to establish a tumor-bearing mouse model. After subcutaneous tumor formation, the tumor volume was determined using calipers. Based on the tumor proliferation curve, tumor proliferation in the DEX treatment group was inhibited from the beginning of treatment, but statistical results showed that there was a significant difference on the 12th day of treatment (Figure 2A). Two days after stopping the drug, the two groups of mice were sacrificed at the same time. The tumor tissues were weighed and statistically processed. The results showed that the tumor weight of the control group was significantly higher than that of the DEX group, and the difference was statistically significant (Figure 2B). This finding indicated that DEX can inhibit the tumor proliferation of tumor-bearing mice consistently, as assessed by tumor volume or tumor mass.
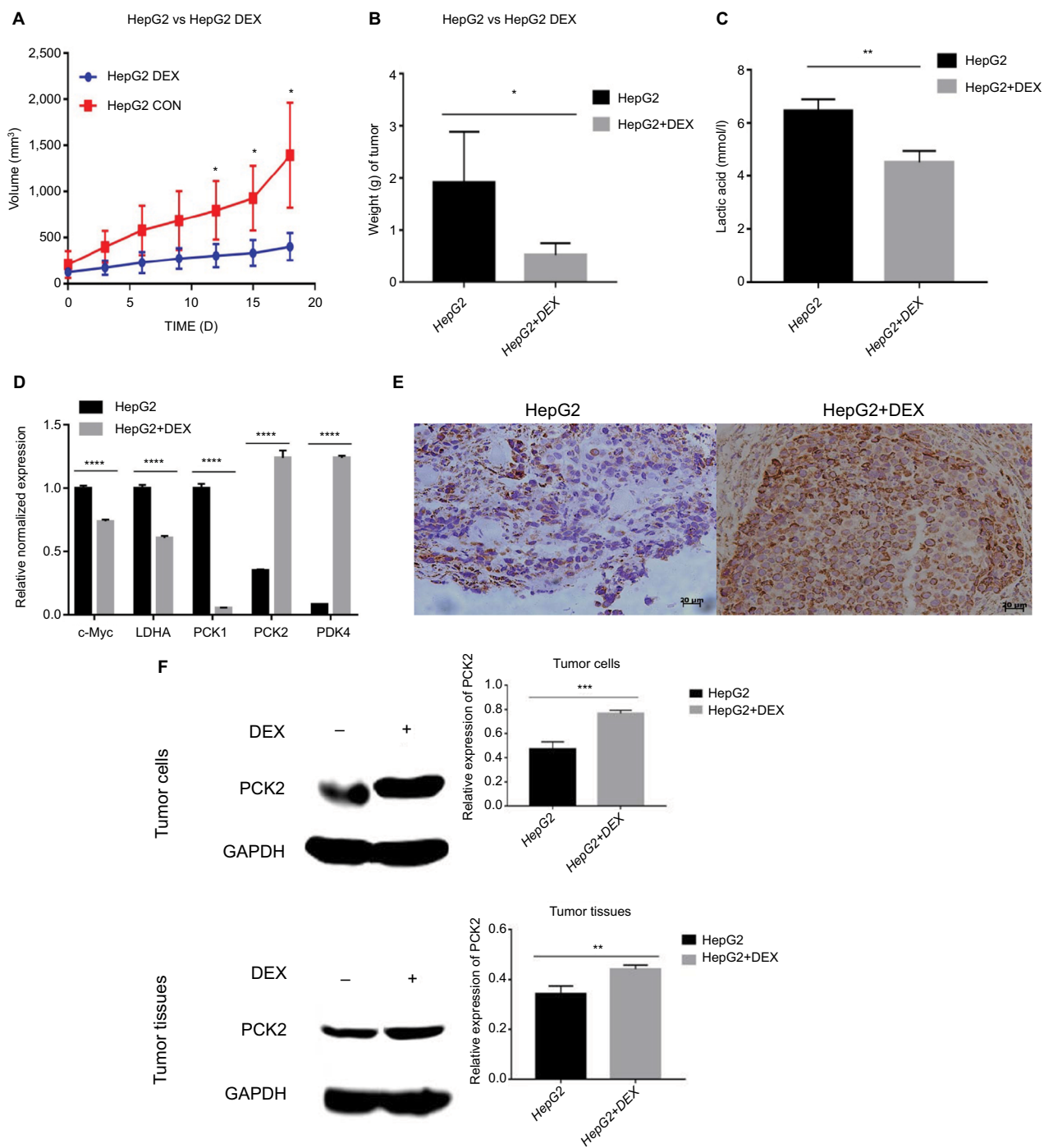
**A** HepG2 vs HepG2 DEX

**B** HepG2 vs HepG2 DEX

**C**

**D**

**E** HepG2    HepG2+DEX

**F**

Figure 2 (*Continued*)

## DEX can inhibit glycolysis in HepG2 cells

The aerobic oxidation of sugar is the same as the reaction step of glycolysis from glucose to pyruvic acid. Aerobic oxidation causes pyruvic acid to enter the mitochondria for the tricarboxylic acid cycle, whereas glycolysis produces pyruvate to produce lactic acid. The basal lactic acid content reflects the degree of glycolysis of the tumor cells to some extent. By measuring the lactic acid content in the medium, we found that the lactic acid content in the HepG2 medium was significantly lower after the DEX treatment. Statistical analysis revealed a statistically significant difference between the two groups (Figure 2C).
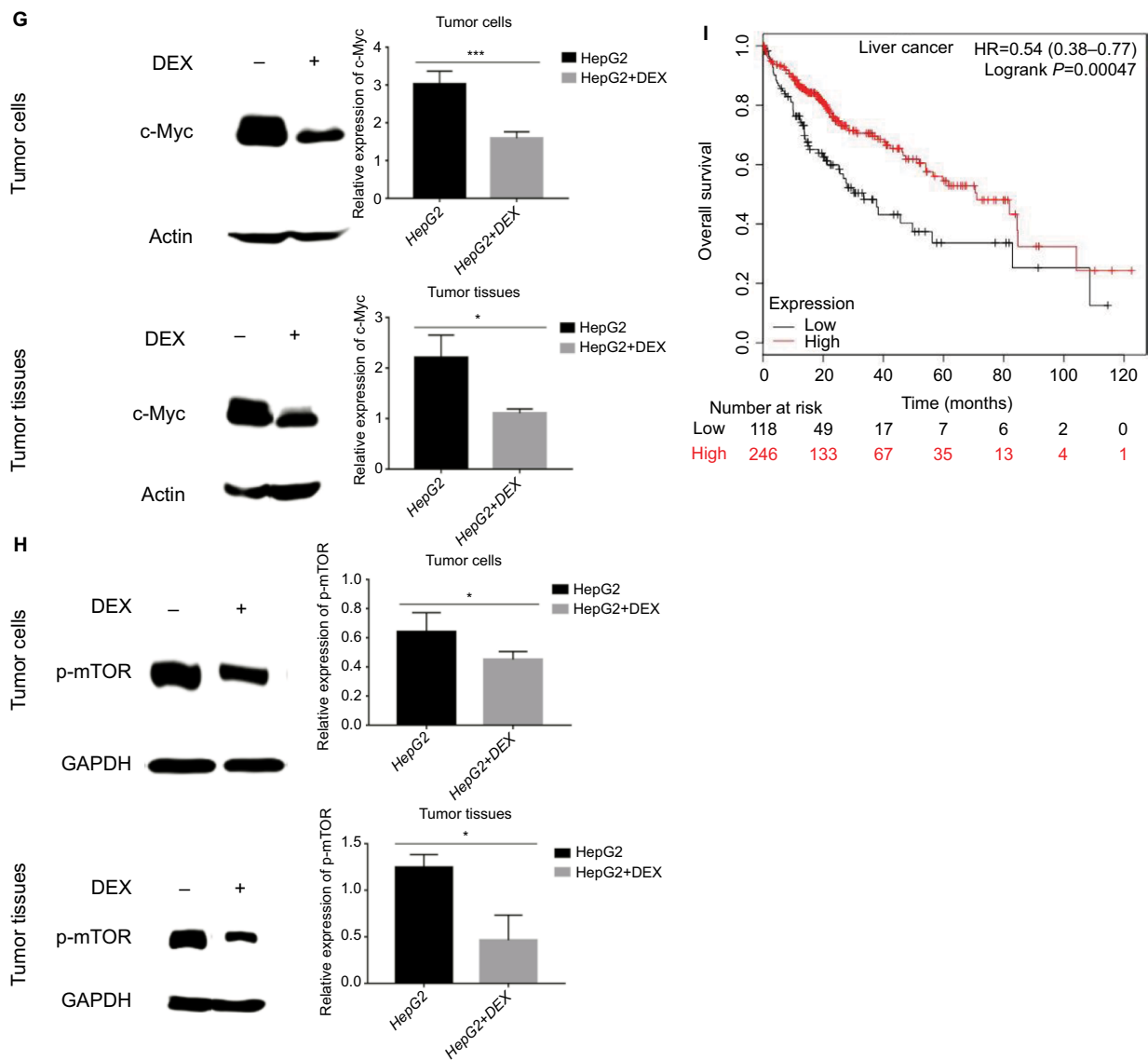
**G**



**H**



**I**



**Figure 2** DEX inhibits HepG2 cells in vivo and its mechanisms.

**Notes:** DEX inhibits the growth of HEPG2 solid tumor volume and weight in vivo. After 12 days of DEX treatment, the difference in solid tumor volume between the control and the DEX groups was statistically significant. At the end of the experiment, solid tumors were weighed, and the difference in solid tumor weight between the control and the DEX groups was statistically significant (**A** and **B**). DEX inhibits the production of lactic acid in a cell culture medium. After DEX treatment, the lactic acid content in the medium was significantly reduced, and the difference was statistically significant, indicating that DEX can inhibit the glycolysis of HepG2 cells (**C**). Detection of expression of genes involved in glucose metabolism by DEX by real-time PCR (**D**). After DEX treatment, the expression of c-Myc, LDHA, and PCK1 in HepG2 cells was significantly decreased, whereas the expression of PCK2 and PDK4 was significantly increased. The difference was statistically significant; detection of the effect of DEX on the expression of PCK2 in HEPG2 xenografts by immunohistochemical (**E**). Western detection of the effect of DEX on PCK2, c-Myc, and p-mTOR in HEPG2 cells and tissues. After treatment with DEX, PCK2 was upregulated, c-Myc was downregulated, and p-mTOR was downregulated in HepG2 cells and solid tumors. The difference was statistically significant (**F–H**). Relationship between expression of PCK2 and patient prognosis of liver cancer in KM plotter database. Hepatocellular carcinoma patients with high expression of PCK2 had longer overall survival than patients with low expression of PCK2. The difference is statistically significant (**I**). All data were analyzed by using the chi-squared test. $P<0.05$ was considered to be significant (*$P<0.05$, **$P<0.01$, ***$P<0.001$, ****$P<0.0001$).

**Abbreviations:** DEX, dexamethasone; p-mTOR, phosphor-mammalian target of rapamycin.

## The molecular mechanism by which DEX inhibits HepG2 proliferation

To further study the molecular changes by which DEX inhibits the proliferation of tumor cells, we extracted total RNA from HepG2 cells treated with 300 µg/mL DEX for 48 hours and untreated HepG2 cells, and we reverse transcribed the RNA into cDNA. The expression of c-Myc was down-regulated by 0.738-fold compared with the control group after HepG2 cells were treated with DEX. The expression of LDHA was downregulated by 0.6064-fold compared with the control group; the expression of PCK2 was upregulated by 3.53-fold higher compared with the control group; and the expression of PCK1 was downregulated by 0.05459-fold compared with the control group; the expression of pyruvate

dehydrogenase kinase isozyme 4 (PDK4) was upregulated by 14.98-fold compared with the control group, and the difference was statistically significant (Figure 2D). In addition, we used immunohistochemical staining of transplanted tumor tissue sections to find that the expression level of PCK2 in the treatment group was significantly higher than that in the control group (Figure 2E). Similarly, at the protein level, we also found that PCK2 was upregulated by 1.59-fold in the DEX group compared with the control group in tumor cells, while PCK2 was upregulated by 1.288-fold in the DEX group compared with the control group at the protein level in the tumor tissue (Figure 2F). To further clarify which signaling pathways affect the tumor's metabolism, we performed Western blot on the tumor cells and tumor tissue proteins. We found that DEX can downregulate c-Myc levels by 0.5276-fold at the protein level in tumor cells, and it can downregulate the c-Myc level by 0.5016 times in the tumor tissue (Figure 2G), we also found that DEX can downregulate p-mTOR levels by 0.7027-fold and 0.3726-fold at the protein level in tumor cells and tissues, respectively (Figure 2H). In addition, the Kaplan–Meier plotter was used to query the metabolic-related genes, and it was found that the downregulation of LDHA, the upregulation of PCK2, and the upregulation of PDK4 were beneficial to prolong the overall survival of patients (Figure S1A, B).

## The expression of PCK2 is closely related to the overall survival of tumor patients

In addition to the upregulation of PCK2 in patients with liver cancer, it is beneficial to prolong the overall survival of patients (Figure 2I). We also investigated the relationship between the expression of PCK2 and the overall survival of patients with ovarian, gastric, and lung cancer (Figure S1C–E). In patients with ovarian cancer, gastric cancer, and lung cancer, those with high expression of PCK2 had a higher overall survival than those with lower PCK2, and the difference was statistically significant.[21]

## DEX can increase the tumor growth of 4T1 tumor mice by regulating immunosuppression

Previous studies have shown that DEX can inhibit the function of the immune system, but because of the lack of T cell immunity in nude mice, the effect of DEX on the immune system cannot be studied in this model, so we used mouse-derived breast cancer cells 4T1 subcutaneously inoculated in immunocompetent mice to determine whether DEX can still inhibit tumor growth under normal immune function. According to the measured long and short diameter of 4T1 tumors, the tumor volume was calculated, and the proliferation curve was drawn. On the ninth day of treatment, the volume difference between the two groups was statistically significant. The tumor volume of the control group was significantly larger than that of the DEX group (Figure 3A). We found that DEX not only inhibits tumor growth in immunodeficient nude mice but also has a role in inhibiting tumor growth in hairy mice with normal immune function.

To further study the effect of DEX on immune cells, two mice in each group were sacrificed on the fourteenth day of the experiment. We found that the spleen size of the tumor-bearing mice was significantly reduced after DEX treatment (Figure 3B), the spleen is the largest immune organ, and its reduction can reflect the immune function of the body. The tumor tissue, spleen tissue, and lymph node tissue near the tumor were taken, and the cells were extracted and analyzed by flow cytometry with different antibody markers. In the lymph nodes near the tumor, the CD4+ T cells/CD45+ cells and CD8+ T cells/CD45+ cells in the lymph nodes of the experimental group was significantly higher than that of the control group (Figure 3C, D, E), Additionally, the content of Treg cells/CD4+ T cells of the experimental group was significantly lower than those of the control group, the difference was statistically significant (Figure 3D, F). We unexpectedly found that the content of MDSCs in the tumor tissue was reduced in the experimental group compared with the control group. The difference was statistically significant (Figure 3G, H). After extracting the tumor tissue, RNA was extracted for real-time PCR, and we found that the tumor-associated inflammatory factors GRANZYME B, IFN- , and IL-1B were significantly downregulated, and IL-10 was significantly upregulated, indicating that DEX has an inhibitory effect on the body's immune system (Figure 3I). From the aforementioned results we believe that although DEX has an inhibitory effect on the body's immune system, it can upregulate the ratio of CD4+ T cells and CD8+ T cells, which inhibit tumor cell growth, while downregulating the proportion of MDSC and Treg cells with immunosuppressive effects.

## Discussion

In the process of tumor cell proliferation, not only a large amount of energy but also a large number of metabolic intermediates, such as nucleic acids, amino acids, and lipids are needed to satisfy the synthesis of substances in the process of
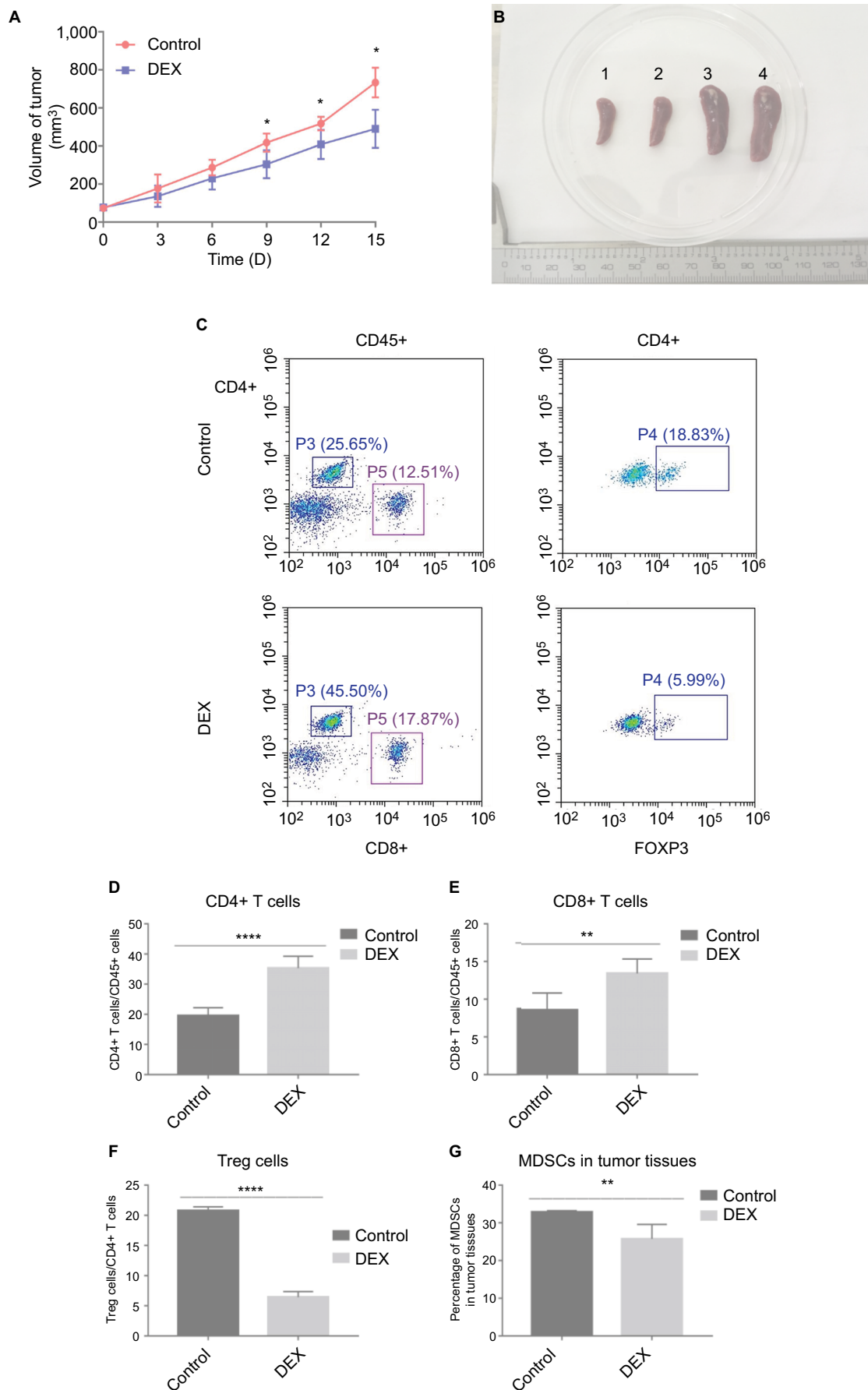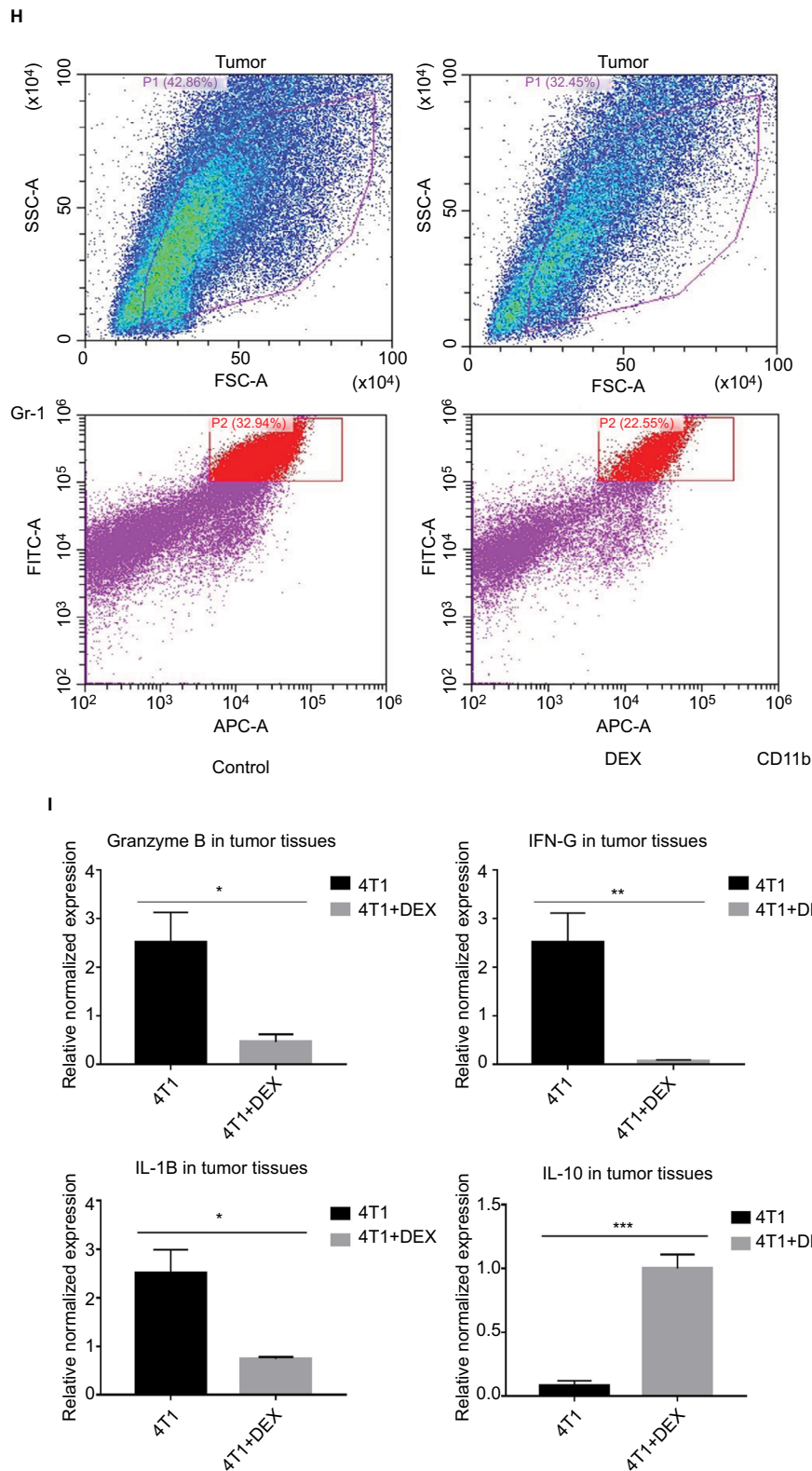
**Figure 3** (*Continued*)

**H**



**I**



**Figure 3** DEX inhibits tumor proliferation by affecting immune cells.
**Note:** DEX inhibits the growth of 4T1 xenografts in vivo. After 9 days of DEX treatment, the volume of transplanted tumors in the control and the DEX groups was statistically significant (**A**). DEX can reduce the spleen of tumor-bearing mice. Spleens 1 and 2 were in the DEX treatment group, and spleens 3 and 4 in the control group (**B**). Effect of DEX on CD4+ T cell, CD8+ T cells, and Treg cells in draining lymph nodes of 4T1 xenografts (**C**) and its statistic graph (**D–F**). After DEX treatment, CD4+/CD45+ and CD8+/CD45+ are upregulated, and Treg cells are downregulated. The MDSCs are downregulated in the tumor tissues, the difference is statistically significant (**G** and **H**). There was an effect of DEX on inflammatory factors in the tumor tissues: positively regulated cytokines like Granzyme B, IFN-$\gamma$, and il-1B were downregulated, and negatively regulated cytokines like IL-10 were upregulated. The difference was statistically significant (**I**). All data were analyzed by using chi-squared test. $P<0.05$ was considered to be significant (*$P<0.05$, **$P<0.01$, ***$P<0.001$, ****$P<0.0001$).
**Abbreviations:** DEX, dexamethasone; IFN, interferon; MDSC, myeloid-derived suppressor cells.

tumor cell proliferation.[2] Although oxidative phosphorylation can produce a large amount of energy, its final metabolites are basically water and carbon dioxide, which cannot provide the necessary raw materials for the synthesis of substances. While aerobic glycolysis produces less energy, the glycolysis process can produce a large number of metabolic intermediates, which can meet the material needs of the tumor cell proliferation process. Therefore, tumor cells provide energy and a large number of metabolic intermediates for their proliferation by enhancing the glycolysis process. Ma et al also used DEX to treat the mouse hepatoma cell line H22. It was found that DEX can upregulate 11b-HSD1 and downregulate 11b-HSD2 to inhibit the proliferation of H22 cells. It was also found that DEX can upregulate G6Pase and PEPCK, which is consistent with our experiment results.[9] Luo et al's study found that the downregulation of PCK2 expression in melanoma-derived cells is responsible for the upregulated malignancy of tumor-regenerating cells. Upregulation of PCK2 can effectively inhibit tumor cell proliferation, and downregulation of PCK1 can reduce the conversion of cytosolic oxaloacetate to phosphoenolpyruvate and increase the conversion to malic acid. Malic acid can be transferred into mitochondria through malate-aspartate transporters, and malic acid is then converted to oxaloacetate and catalyzed by PCK2 to form phosphoenol pyruvate, so the effect of PCK2 on gluconeogenesis is more obvious than that of PCK1, similar to the results of our experiments.[3] Sun et al found that activation of mTOR can mimic hypoxia effects by inducing expression of HIF1-α, which, in turn, enhances glycolytic enzymes by collaborating with c-Myc-heterogeneous nuclear ribonucleoproteins splicing regulators, this contributes to the Waberg effect.[10] Toschi et al found that phospholipase D-mTOR signaling is very common in cancer and essential for the conversion of metabolism to aerobic glycolysis.[11] Hsieh et al believe that Myc transcriptional and posttranscriptional regulation and the interaction between Myc and mTOR are critical for the metabolism and rapid growth of tumor cells.[12] In our study, after DEX treatment, the expression levels of phosphorylated mTOR and c-Myc in Hepg2 cells were significantly downregulated at the RNA and protein levels, which affected the activity of glycolytic enzymes, such as the upregulation of PCK2, and the downregulation of LDHA, as well as the downregulation of other factors, which leads to a decrease in the level of aerobic glycolysis of tumor cells, and inhibits the proliferation of tumor cells.

The tumor microenvironment is the internal environment on which tumor cells depend for survival and development. The tumor microenvironment contains a large number of immune cells, such as T lymphocytes, Treg cells, dendritic cells, tumor-associated macrophages, tumor-associated fibroblasts, and MDSCs.[13,14] Among immune cells, CD4+ T cells and CD8+ T cells are recognized as anti-tumor immune cells, which kill tumor cells by releasing anti-tumor cytokines, such as γ-interferon, perforin, and granzyme B.[15,16] Dendritic cells can present tumor-associated antigens to CD8+ T cells to promote the proliferation and activation of T cells and exert anti-tumor effects. Treg cells can produce an immunosuppressive environment by secreting transforming growth factor beta and IL-10, attenuating the anti-tumor effects produced by CD4+ T cells, CD8+ T cells and NK cells.[17–19] Tumor-associated macrophages can act on tumor cells through chemokines, growth factors, and angiogenic factors, thereby promoting tumor growth, invasion, and metastasis. MDSCs are a group of immunosuppressive cells that participate in anti-tumor immunosuppression and promote the immune escape of tumor cells.[20] When we studied whether DEX has anti-tumor effects in normal immunized mice, it was unexpectedly discovered that DEX can increase the ratio of CD4+ T cells and CD8+ T cells in the draining lymph nodes near the tumor, and reduce the proportion of Treg cells in the draining lymph nodes near the tumor; in addition, we found that DEX can reduce the proportion of MDSC in tumor tissues, and there is no significant change in B cells, NK cells, and macrophages; it may be the reason why DEX still has anti-tumor effect in normal mice. Although research on tumor aerobic glycolysis and the tumor immunoinflammatory microenvironment is still ongoing, the results are not satisfactory. Therefore, research on tumor metabolism and the immune microenvironment still needs to be carried out. Of course, due to the wide-ranging effects of DEX and its long-term side effects, it is not feasible to use DEX alone to treat tumors, but we can use DEX to affect tumor glycolysis and the immune cells around tumor tissues. These two aspects would promote the efficacy of certain chemotherapeutic drugs, and we also believe that PCK2 is a promising therapeutic target, since cancer can be treated by upregulating PCK2.

## Acknowledgments

## Disclosure

The authors report no conflicts of interest in this work.

# References

1. Hanahan D, Weinberg RA. Hallmarks of cancer: the next generation. *Cell*. 2011;144(5):646–674.
2. Vander Heiden MG, Cantley LC, Thompson CB. Understanding the Warburg effect: the metabolic requirements of cell proliferation. *Science*. 2009;324(5930):1029–1033.
3. Luo S, Li Y, Ma R, et al. Downregulation of PCK2 remodels tricarboxylic acid cycle in tumor-repopulating cells of melanoma. *Oncogene*. 2017;36(25):3609–3617.
4. Liu YX, Zhang SF, Ji YH, Guo SJ, Wang GF, Zhang GW. Whole-exome sequencing identifies mutated PCK2 and HUWE1 associated with carcinoma cell proliferation in a hepatocellular carcinoma patient. *Oncol Lett*. 2012;4(4):847–851.
5. Meng-Xi Liu LJ. Metabolic reprograming by PCK1 promotes TCA cataplerosis, oxidative stress and apoptosis in liver cancer cells and suppresses hepatocellular carcinoma. *Oncogene*. 2017;10:1038.
6. Shi H, Fang R, Li Y, et al. The oncoprotein HBXIP suppresses gluconeogenesis through modulating PCK1 to enhance the growth of hepatoma cells. *Cancer Lett*. 2016;382(2):147–156.
7. Xian ZY, Liu JM, Chen QK, et al. Inhibition of LDHA suppresses tumor progression in prostate cancer. *Tumour Biol*. 2015;36(10):8093–8100.
8. Chen H, Chen Y, Liu H, Que Y, Zhang X, Zheng F. Integrated expression profiles analysis reveals correlations between the IL-33/ST2 Axis and CD8^{+} T cells, regulatory T cells, and myeloid-derived suppressor cells in soft tissue sarcoma. *Front Immunol*. 2018;9:1179.
9. Ma R, Zhang W, Tang K, et al. Switch of glycolysis to gluconeogenesis by dexamethasone for treatment of hepatocarcinoma. *Nat Commun*. 2013;4:2508.
10. Sun Q, Li S, Wang Y, et al. Phosphoglyceric acid mutase-1 contributes to oncogenic mTOR-mediated tumor growth and confers non-small cell lung cancer patients with poor prognosis. *Cell Death Differ*. 2018;25(6):1160–1173.
11. Toschi A, Lee E, Thompson S, et al. Phospholipase D-mTOR requirement for the Warburg effect in human cancer cells. *Cancer Lett*. 2010;299(1):72–79.
12. Hsieh AL, Walton ZE, Altman BJ, Stine ZE, Dang CV. MYC and metabolism on the path to cancer. *Semin Cell Dev Biol*. 2015;43:11–21.
13. Engblom C, Pfirschke C, Pittet MJ. The role of myeloid cells in cancer therapies. *Nat Rev Cancer*. 2016;16(7):447–462.
14. Chen DS, Mellman I. Oncology meets immunology: the cancer-immunity cycle. *Immunity*. 2013;39(1):1–10.
15. Petrelli A, van Wijk F. CD8(+) T cells in human autoimmune arthritis: the unusual suspects. *Nat Rev Rheumatol*. 2016;12(7):421–428.
16. Jacquin E, Apetoh L. Cell-intrinsic roles for autophagy in modulating CD4 T cell functions. *Front Immunol*. 2018;9:1023.
17. Kato T, Noma K, Ohara T, et al. Cancer-associated fibroblasts affect intratumoral CD8(+) and FoxP3(+) T cells via interleukin 6 in the tumor microenvironment. *Clin Cancer Res*. 2018;24(19):4820–4833.
18. Frydrychowicz M, Boruczkowski M, Kolecka-Bednarczyk A, Dworacki G. The dual role of treg in cancer. *Scand J Immunol*. 2017;86(6):436–443.
19. Chen C, Chen D, Zhang Y, et al. Changes of CD4+CD25+FOXP3+ and CD8+CD28- regulatory T cells in non-small cell lung cancer patients undergoing surgery. *Int Immunopharmacol*. 2014;18(2):255–261.
20. Liu Y, Wei G, Cheng WA, et al. Targeting myeloid-derived suppressor cells for cancer immunotherapy. *Cancer Immunol Immunother*. 2018;67(8):1181–1195.
21. Lánczky A, Nagy Á, Bottai G. miRpower: a web-tool to validate survival-associated miRNAs utilizing expression data from 2,178 breast cancer patients. *Breast Cancer Res Treat*. 2016;160(3):439–446.
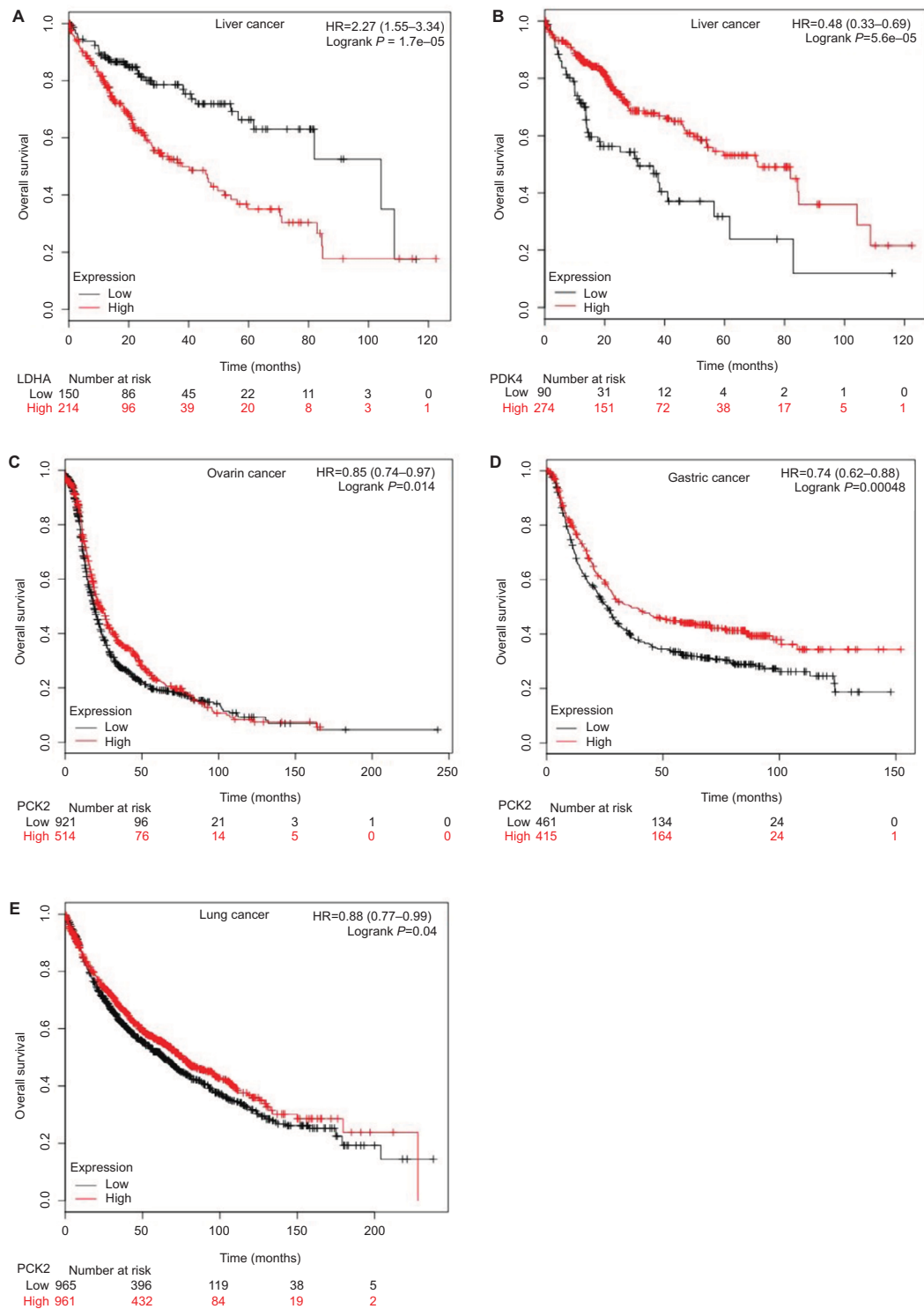
# Supplementary material



**Figure S1** Kaplan–Meier survival curves of overall survival in patients with different cancers. Liver cancer patients with LDHA-low expression have a longer overall survival compared with those with LDHA-high expression (**A**). Liver cancer patients with PDK4-high expression have a longer overall survival compared with those with PDK4-low expression (**B**). Ovarian cancer patients with PCK2-high expression have a longer overall survival compared with those with PCK2-low expression (**C**). Gastric cancer patients with PCK2-high expression have a longer overall survival compared with those with PCK2-low expression (**D**). Lung cancer patients with PCK2-high expression have a longer overall survival compared with those with PCK2-low expression (**E**). The samples in different cancers cohort with top 50% expression levels for different proteins were grouped as high and those with bottom 50% were grouped as low.
**Abbreviation:** LDHA, lactate dehydrogenase A.